

# Device simulations: Reducing non-radiative recombination losses for achieving >15% efficient lead sulfide quantum dot solar cells

Dandan Wang<sup>1</sup>, Chao Ding<sup>1</sup>, Meibo Xing<sup>2</sup>, Haifeng Wu<sup>2</sup>, Ruixiang Wang<sup>2</sup>, and Qing Shen<sup>1\*</sup>

1 Faculty of Informatics and Engineering, The University of Electro Communications, 1-5-1 Chofugaoka, Chofu, Tokyo 182-8585, Japan (\*Corresponding Author); 2 School of Environment and Energy Engineering, Beijing University of Civil Engineering and Architecture, Beijing 100044, PR China

## ABSTRACT

Lead sulfide quantum dots solar cells (PbS QDSCs) have recently received substantial attention due to their unparalleled photoelectric properties that can lead to a new record theoretical efficiency in thin film photovoltaic devices. However, the high voltage losses of PbS QDSCs induced by non-radiative recombination losses bring about the low device performance. In this study, a real planar heterojunction PbS QD-based solar cell structure of FTO/PbS-EMII/PbS-EDT/Au is successfully simulated and then theoretically analyzed the effects of these determining factors on device performance via drift-diffusion modeling. After modulating these factors, a new device is finalized with defect density ( $N_t$ ) of  $10^{15} \text{ cm}^{-3}$  in absorber layer and acceptor density ( $N_A$ ) of  $10^{18} \text{ cm}^{-3}$  in hole transport material (HTM) as well as surface recombination velocity of  $10 \text{ cm}\cdot\text{s}^{-1}$  at absorber/HTM interface, which can deliver a power conversion efficiency (PCE) of 17.08%, with a 27.21% improvement in open-circuit voltage ( $V_{OC}$ ). This method used in this study can provide access guidelines and accelerate the efficiency improvements in PbS QDSCs.

**Keywords:** voltage-loss, non-radiative recombination loss, power conversion efficiency

## NONMENCLATURE

### Abbreviations

$V_{OC}$	Open-circuit voltage
$J_{SC}$	Short-circuit current
FF	Fill factor
PCE	Power conversion efficiency
$V_{loss}$	Voltage loss
$V_{bi}$	Built-in potential
$E_g$	Band gap

$R_s$	Series resistance
$R_{sh}$	Shunt resistance
FTO	Fluorine-doped tin oxide
EMII	1-ethyl-3-methylimidazolium iodide
EDT	1,2-ethanedithiol
ZnO	Zinc oxide
BC	Back junction
<i>Symbols</i>	
$E_c$ and $E_v$	Conduction band minimum and valence band maximum
$N_A$ and $N_D$	Acceptor concentration and donor concentration
$N_t$	Defect density
$S_n$	Recombination velocity
$q$	Elementary charge

## 1. INTRODUCTION

It is critical to developing and utilizing renewable energy resources to realize the aim of carbon neutrality by 2050. Low-cost and solution-processed lead sulfide quantum dot solar cells (PbS QDSCs) are the devices providing renewable clean energy, which have received remarkable attention for the third-generation solar cell applications owing to their huge exciton Bohr radius (Wise, 2000; Zhou, Itoh, Uemura, Naka, & Chujo, 2002), wide absorption spectrum (Bi et al., 2018) and the possibility of multiple exciton effect (Haipeng Lu, 2020; Wise, 2000). The state-of-the-art PbS QDSC has reached a certified power conversion efficiency (PCE) of 12.43% (Sun et al., 2020) for the combinations of surface chemistry and device architecture optimizations (Lim et al., 2019; Liu, Xian, Ye, & Zhou, 2021). However, PbS QDSCs still have relatively low PCEs compared with the state-of-the-art GaAs (27.8%) thin-film single-junction solar cells ("https://www.nrel.gov/pv/cell-efficiency.html"). The main factor that limits the

efficiency of PbS QDSCs is the large voltage loss ( $V_{\text{loss}} = E_g/q - V_{\text{OC}}$ ,  $E_g$  is the band gap and  $q$  is elementary charge), the achieved PCE has a  $V_{\text{loss}}$  over 600 mV in the state-of-the-art of PbS QDSCs, implying that there is still much room to increase open-circuit voltage ( $V_{\text{OC}}$ ) of PbS QDSCs.

There is a lot of experimental and theoretical researches on  $V_{\text{OC}}$  enhancement. The decrease of  $V_{\text{OC}}$  is typically interrelated to defect-assisted recombination losses in PbS QDSCs (Zhang et al., 2020). The chemical passivation and doping engineering have not only experimentally utilized to reduce QD surface defect sites but favored solar cell structures to maximize carrier extraction (Kirmani, Luther, Abolhasani, & Amassian, 2020; Lee et al., 2020). In addition, the modulations of recombination losses in bulk materials and at interfaces are also paramount to enhance  $V_{\text{OC}}$  and to further optimize the device degradation induced by defects (Kemp et al., 2013).

To compute the performance limit of this photovoltaic device, we fabricated 16 same PbS QDSCs with typical n-i-p device structures under similar conditions and simultaneously. The experimental values are compared with drift-diffusion simulation results as shown in Fig.1. And then, the device performance impacting factors were theoretically investigated. After optimizing these parameters, a new efficiency record of 17.08% can be obtained, with  $V_{\text{OC}}$  of 751.90mV, short-circuit current ( $J_{\text{sc}}$ ) of 30.04 mA/cm<sup>2</sup>, and fill factor (FF) of 69.58%.

## 2. EXPERIMENT AND SIMULATION

### 2.1 Device fabrication

The real PbS QD-based solar cells possess the n-i-p planar heterojunction structure of ITO/ZnO/PbS-1-ethyl-3-methylimidazolium iodide (EMII)/PbS-1,2-ethanedi-thiol (EDT)/Au, which was fabricated according to our previous work (Ding et al., 2020). In brief, the light-harvesting PbS QDs are obtained through pure iodine passivation during ligand exchange as solar absorber, which has a 200 nm thickness sandwiched between Zinc oxide (ZnO), and PbS-EDT. The electron transport material, ZnO nanocrystals with a 100 nm thickness layer, are deposited on Fluorine-doped tin oxide (FTO), and the hole transport material, PbS-EDT with a 130 nm thickness layer, are fabricated via layer-by-layer spin-coating on top of PbS-EMII absorption layer. Through device characterization and measurement, 16 same devices have an average PCE of 9.56% with a  $V_{\text{OC}}$  of 0.59 V. The  $E_g$  of solar absorption

materials in this type of PbS QDSCs is 1.31 eV, however, the performance parameters of these devices remain lower than these corresponding theoretical efficiency limits (PCE of 33.28% with a  $V_{\text{OC}}$  of 1.05 V) (Shockley & Queisser, 1961).

### 2.2 Device simulation parameters

The device simulations were performed through One-dimensional Solar Cell Capacitance Simulator (SCAPS-1D) ver. 3.3.10 software which is developed by Gent university (M. Burgelman, 2000). This method can be used to design PbS QD-based solar cell so that its performance investigations can be implemented via varying material parameters. To obtain the realistic situation of the real PbS QD-based solar cell device, it needs to supply reliable material properties inputting into device simulations. Therefore, the material parameters used in device calibration are obtained from the literatures (Ding et al., 2020; Lin et al., 2021) or from simulation fitting. The experimental device has the structure of FTO (300 nm)/ZnO (100 nm)/PbS-EMII (200 nm)/PbS-EDT (130 nm)/Au (100 nm), and its corresponding energy level diagram is shown in Fig.1(b). All simulations were performed at 300 K operation temperature and AM 1.5G illumination.

## 3. RESULTS AND DISCUSSION

### 3.1 Device simulation

In this section, a simulated device has been obtained via SCAPS-1D approach (Fig.1(a)). The ideal factor ( $n_{\text{ID}}$ ) of 1.56 in the first simulation is calculated from  $V_{\text{OC}} = n_{\text{ID}} k_B T \ln(J_{\text{ph}}/J_0)/q$ , where  $J_0$  and  $J_{\text{ph}}$  are dark saturation current and light-generated current, respectively,  $n_{\text{ID}} k_B T/q$  is defined as the thermal voltage (Fig.1(c)). This value is close to that of the experimental device ( $n_{\text{ID}} = 1.60$ ) (Ding et al., 2020). It suggests that the dominant nature of recombination in the first simulated device (Simulation 1) is the trap-assisted recombination. The total non-radiative recombination is comprised of bulk absorber recombination and interface recombination (Raoui, Kazim, Galagan, Ez-Zahraouy, & Ahmad, 2021). Furthermore, the power law dependence of  $J_{\text{sc}}$  upon the illumination intensity can be calculated following  $J_{\text{sc}} \sim I^\alpha$ , the exponential factor ( $\alpha$ ) approaches to unity (Fig. 1(c)), which indicated that the charge efficiency collection is independent of light intensity. Additionally, the equivalent circuit model (Hu et al., 2016; Mandelis, Hu, & Wang, 2016) was used to qualitatively measure the impacts of series resistance ( $R_s$ ) (2.57  $\Omega \cdot \text{cm}^2$ ) and recombination resistance ( $R_{\text{rec}}$ )

(71.96  $\Omega\cdot\text{cm}^2$ ) inside device (Fig.1 (d)), it is revealed that the poor recombination resistance brings about the low device performance. In this study, it is considered that all of the above-described recombination losses to design highly efficient PbS QDSCs.

### 3.2 Effect of non-radiative recombination losses

The defect density in the absorber layer is a key element to enhance solar cell performance which can be obtained from the QD film's quality. The typical measured defect density for PbS QD films ranges from  $10^{16}$  to  $10^{18}$   $\text{cm}^{-3}$  (Ding et al., 2020; Wang et al., 2019), which is higher than that of other inspiring materials ( $\sim 10^{13}$   $\text{cm}^{-3}$ ) (Lu, Biesold-McGee, Liu, Kang, & Lin, 2020; Ng et al., 2019). The layer-to-layer preparation of PbS-EMII absorber material and PbS-EDT hole transport material (HTM) can improve the formation probability of the absorber/HTM interface defect. The absorber/HTM interface recombination is one of the main sources of poor stability and performance in the PbS QDSCs (Liu et al., 2021; Muhibullah Al Mubarak, 2020). From previously literature, the electron transport material (ETM)/absorber interface defect recombination can be neglectable as compared to the above-mention two non-radiative recombination rates (Lin et al., 2021).

To explore the influence of defect density ( $N_t$ ) in the absorber layer on device characteristics to gain the

optimum value for PbS-EMII film, the  $N_t$  is varied from  $10^{17}$  to  $10^{11}$   $\text{cm}^{-3}$  as shown in Fig.2(a). It is found that the performance parameters have exponentially improved up to  $N_t=10^{16}$   $\text{cm}^{-3}$  as the decrease in  $N_t$ , afterword these performance parameters enhanced gradually and approached maximum value at  $N_t=10^{15}$   $\text{cm}^{-3}$  (Simulation 2), thus yielding a PCE of 10.65%, with a  $V_{OC}$  enhancement of 3.54%. It is revealed that the resistive losses ( $R_s=2.57$   $\Omega\cdot\text{cm}^2$  and  $R_{rec}=72.75$   $\Omega\cdot\text{cm}^2$ ) and ideal factor ( $n_{ID}=1.57$ ) in the Simulation 2 are slightly ameliorated when they are compared to the Simulation 1 (Fig.2(d,e)). Moreover, the absorber defect optimization has no obvious impacts on the  $qV_{bi}$  (0.638 eV) across the absorber layer (Fig.2(f)).

Moreover, the high acceptor concentration ( $N_A$ ) in HTM is more useful to yield band tilt/bending for intrinsic solar absorber. With the enhancement of  $N_A$  in HTM ( $10^{16}$ - $10^{18}$   $\text{cm}^{-3}$ ), an increment in PCE from 10.65% to over 13% can be realized. The  $V_{OC}$  increase to 0.70 V because of the  $V_{bi}$  value enlarged to 0.85 V in the Simulation 3 ( $N_A$  of  $10^{18}$   $\text{cm}^{-3}$  in HTM layer) (Fig.2(b)). There is also a similar increase in  $R_{rec}$  value (781.10  $\Omega\cdot\text{cm}^2$ ) in the Simulation 3 which can impede current leakage caused by surface recombination. On the other hand, high doping concentration can introduce unavoidable deep trap states in HTM materials (Rahul Pandeya, 2020) and to augment  $R_s$  (2.84  $\Omega\cdot\text{cm}^2$ ) (Fig.2(e)).

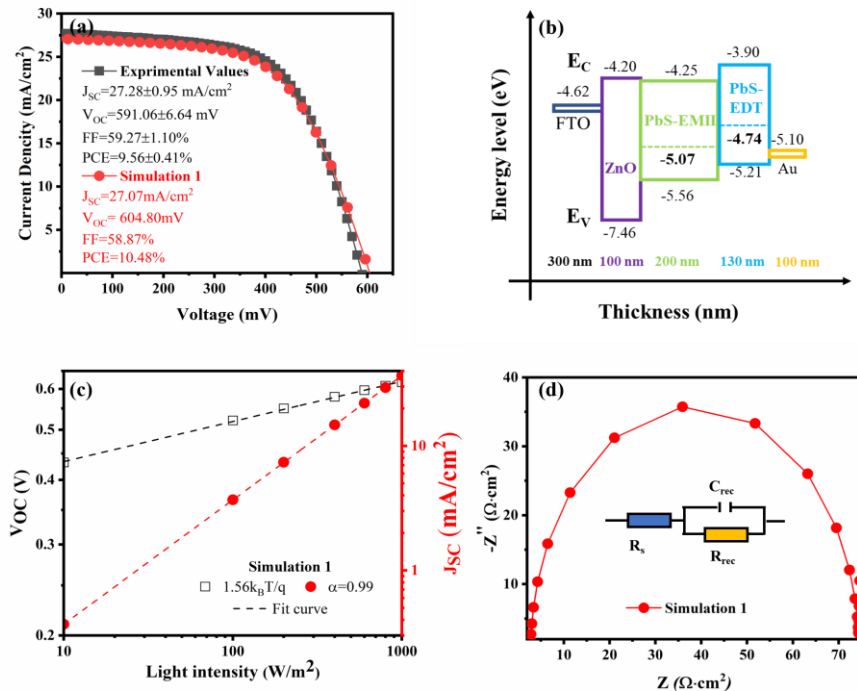


Fig. 1. Corresponding J-V curve (a), Energy band level (b), light intensity dependence on  $V_{oc}$  and  $J_{sc}$  (c) and Nyquist plot (d).

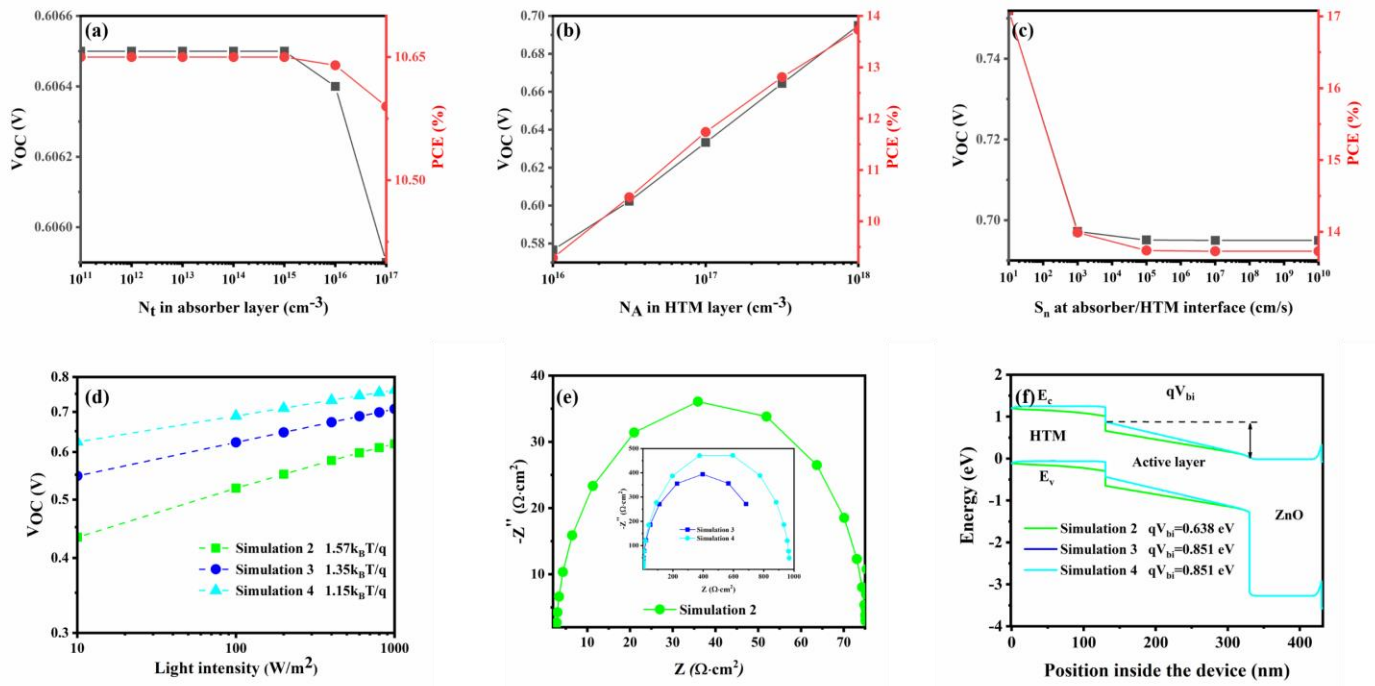


Fig. 2. Trap density in absorber layer (a), Acceptor density in HTM (b) and recombination velocity at absorber/HTM interface (c) influences on  $V_{OC}$  and PCE; light intensity dependence on  $V_{OC}$  (d), Nyquist plot (e) and energy band diagram (f) of Simulation 2, Simulation 3 and Simulation 4.

Furthermore, modulating recombination velocity at absorber/HTM interface,  $S_n$ , ( $10^{10} - 10^1 \text{ cm}^{-1}\text{s}^{-1}$ ) (Fig.2(c)), the values of  $R_s$  and  $R_{rec}$  are ameliorated ( $R_s=2.56 \Omega\cdot\text{cm}^2$ ,  $R_{rec}=967.70 \Omega\cdot\text{cm}^2$ ) and thus bringing to a big increment in  $J_{SC}$  ( $30.04 \text{ mA}/\text{cm}^2$ ), small enhancement in PCE (17.08%),  $V_{OC}$  (0.75 V) and FF (69.58%), and a stable  $qV_{bi}$  value (0.851 eV) (Fig.2(f)) in the Simulation 4 ( $S_n=10 \text{ cm}^{-1}\text{s}^{-1}$ ). Through these optimizations, it is found that ameliorating the bulk and interface trap-assisted recombination rates can significantly reduce non-radiative recombination losses ( $n_{ID}=1.15$ , Fig.2(d)) via enhancing the lifetime and diffusion length of charges inside device (Raoui et al., 2021), and thus improving carrier collection probability at ETM/absorber and absorber/HTM interfaces.

In a summary, reducing interface and absorber defect densities is recommended to design high-performance PbS QDSCs. From the perspective of experiment, the interaction mechanism between bulk materials and surfactants are vital to enhance the device performance and stability (Lee et al., 2020; Mohan Yuan, 2021). Additionally, it also needs that controlling suitable doping concentration in HTM modifies the HTM Fermi level and ameliorates charge-transport properties (A. R. Kirmani, F. P. G. de Arquer, & T. Wu, 2018).

#### 4. CONCLUSION

The voltage losses caused by non-radiative recombination losses were theoretically analyzed with the n-i-p planar heterojunction structure via drift-diffusion modeling. It is unraveled that reducing resistive losses caused by trap-assisted recombination is critical to enhance  $V_{OC}$  value in PbS QDSCs. Moreover, the absorber defect density and HTM acceptor density should not be higher than  $10^{15} \text{ cm}^{-3}$  and  $10^{18} \text{ cm}^{-3}$ , respectively, as well as the interface recombination velocity at absorber/HTM should approach to  $10^1 \text{ cm}^{-1}\text{s}^{-1}$ , these strategies can deliver a new PCE record over 15%.

#### ACKNOWLEDGEMENT

This research was supported by the Japan Science, Technology Agency (JST) Mirai program (JPMJMI17EA), MEXT KAKENHI Grant (26286013, 17H02736) and Beijing University of Civil Engineering and Architecture scientific research ability improvement plan of young teachers (No. Z21045).

## REFERENCE

- [1] A. R. Kirmani, A. D. S., M. R. Niazi, M. A. Haque, M. Liu, F. P. G. de Arquer, J. X., B. Sun, O. Voznyy, N. Gasparini, D. Baran, & T. Wu, E. H. S., A. A. Amassian. (2018). Overcoming the Ambient Manufacturability-Scalability Performance Bottleneck in Colloidal Quantum Dot Photovoltaics. *Adv. Mater.*, 30, 1801661. doi:10.1002/adma.201801661
- [2] Bi, Y., Pradhan, S., Gupta, S., Akgul, M. Z., Stavrinadis, A., & Konstantatos, G. (2018). Infrared Solution-Processed Quantum Dot Solar Cells Reaching External Quantum Efficiency of 80% at 1.35 microm and Jsc in Excess of 34 mA cm<sup>-2</sup>. *Adv. Mater.*, 30(7). doi:10.1002/adma.201704928
- [3] Ding, C., Liu, F., Zhang, Y., Hayase, S., Masuda, T., Wang, R., . . . Shen, Q. (2020). Passivation Strategy of Reducing Both Electron and Hole Trap States for Achieving High-Efficiency PbS Quantum-Dot Solar Cells with Power Conversion Efficiency over 12%. *ACS Energy Lett.*, 3224-3236. doi:10.1021/acscenergylett.0c01561
- [4] Haipeng Lu, Z. H., Marissa S. Martinez, Justin C. Johnson ORCID logo, Joseph M. Luther and Matthew C. Beard. (2020). Transforming Energy Using Quantum Dots. *Energy Environ. Sci.*, 13, 1347-1376. doi:10.1039/C9EE03930A
- [5] NREL, Research Cell Record Efficiency Chart, National Renewable Energy Laboratory, <https://www.nrel.gov/pv/cell-efficiency.html>, accessed August 2019.
- [6] Hu, L., Mandelis, A., Lan, X., Melnikov, A., Hoogland, S., & Sargent, E. H. (2016). Imbalanced charge carrier mobility and Schottky junction induced anomalous current-voltage characteristics of excitonic PbS colloidal quantum dot solar cells. *Sol. Energy Mat. Sol. C.*, 155, 155-165. doi:10.1016/j.solmat.2016.06.012
- [7] Kemp, K. W., Labelle, A. J., Thon, S. M., Ip, A. H., Kramer, I. J., Hoogland, S., & Sargent, E. H. (2013). Interface Recombination in Depleted Heterojunction Photovoltaics based on Colloidal Quantum Dots. *Adv. Energy Mater.*, 3(7), 917-922. doi:10.1002/aenm.201201083
- [8] Kirmani, A. R., Luther, J. M., Abolhasani, M., & Amassian, A. (2020). Colloidal Quantum Dot Photovoltaics: Current Progress and Path to Gigawatt Scale Enabled by Smart Manufacturing. *ACS energy lett.*, 5(9), 3069-3100. doi:10.1021/acscenergylett.0c01453
- [9] Lee, H., Yoon, D. E., Koh, S., Kang, M. S., Lim, J., & Lee, D. C. (2020). Ligands as a universal molecular toolkit in synthesis and assembly of semiconductor nanocrystals. *Chem. Sci.*, 11(9), 2318-2329. doi:10.1039/c9sc05200c
- [10] Lim, H., Kim, D., Choi, M. J., Sargent, E. H., Jung, Y. S., & Kim, J. Y. (2019). Suppressing Interfacial Dipoles to Minimize Open - Circuit Voltage Loss in Quantum Dot Photovoltaics. *Adv. Energy Mater.*, 9(48). doi:10.1002/aenm.201901938
- [11] Lin, W. M. M., Yazdani, N., Yarema, O., Yarema, M., Liu, M., Sargent, E. H., . . . Wood, V. (2021). Recombination Dynamics in PbS Nanocrystal Quantum Dot Solar Cells Studied through Drift-Diffusion Simulations. *ACS Appl. Electron. Mater.*, 3(11), 4977-4989. doi:10.1021/acsaem.1c00787
- [12] Liu, J., Xian, K., Ye, L., & Zhou, Z. (2021). Open - Circuit Voltage Loss in Lead Chalcogenide Quantum Dot Solar Cells. *Adv. Mater.*, 33(29). doi:10.1002/adma.202008115
- [13] Lu, C. H., Biesold-McGee, G. V., Liu, Y., Kang, Z., & Lin, Z. (2020). Doping and ion substitution in colloidal metal halide perovskite nanocrystals. *Chem. Soc. Rev.*, 49(14), 4953-5007. doi:10.1039/c9cs00790c
- [14] M. Burgelman, P. N., S. Degraeve. (2000). Modeling polycrystalline semiconductor solar cells. *Thin Solid Films*, 361-362, 527-532.
- [15] Mandelis, A., Hu, L., & Wang, J. (2016). Quantitative measurements of charge carrier hopping transport properties in depleted-heterojunction PbS colloidal quantum dot solar cells from temperature dependent current-voltage characteristics. *RSC Adv.*, 6(95), 93180-93194. doi:10.1039/c6ra22645k
- [16] Mohan Yuan, X. W., Xiao Chen, Jungang He, Kanghua Li, Boxiang Song, Huicheng Hu, Liang Gao, Xinzheng Lan, Chao Chen, and Jiang Tang. (2021). Phase-Transfer Exchange Lead Chalcogenide Colloidal Quantum Dots: Ink Preparation, Film Assembly, and Solar Cell Construction. *Small*, 2102340, 1-17. doi:10.1002/smll.202102340
- [17] Muhibullah Al Mubarak, H. A., Febrian Tri Adhi Wibowo, Wooseop Lee, Hyung Min Kim, Du Yeol Ryu, Ju-Won Jeon, and Sung-Yeon Jang. (2020). Molecular Engineering in Hole Transport  $\pi$ -Conjugated Polymers to Enable High Efficiency Colloidal Quantum Dot Solar Cells. *Adv. Energy Mater.*, 1902933. doi:10.1002/aenm.201902933
- [18] Ng, C. H., Nishimura, K., Ito, N., Hamada, K., Hirotsu, D., Wang, Z., . . . Hayase, S. (2019). Role of

- Gel 2 and SnF 2 additives for SnGe perovskite solar cells. *Nano Energy*, 58, 130-137. doi:10.1016/j.nanoen.2019.01.026
- [19] Rahul Pandeya, A. K., Karanveer Singhb, Sumit Kumar Patelb, Hardeep Singhb, Jaya Madan. (2020). Device simulations: Toward the design of >13% efficient PbS colloidal quantum dot solar cell. *Solar Energy*, 207 893–902. doi:10.1016/j.solener.2020.06.099
- [20] Raoui, Y., Kazim, S., Galagan, Y., Ez-Zahraouy, H., & Ahmad, S. (2021). Harnessing the potential of lead-free Sn–Ge based perovskite solar cells by unlocking the recombination channels. *Sustain. Energy Fuels*. doi:10.1039/d1se00687h
- [21] Shockley, W., & Queisser, H. J. (1961). Detailed Balance Limit of Efficiency of p - n Junction Solar Cells. *J. Appl. Phys.*, 32(3), 510-519. doi:10.1063/1.1736034
- [22] Sun, B., Johnston, A., Xu, C., Wei, M., Huang, Z., Jiang, Z., . . . Sargent, E. H. (2020). Monolayer Perovskite Bridges Enable Strong Quantum Dot Coupling for Efficient Solar Cells. *Joule*, 4(7), 1542-1556. doi:10.1016/j.joule.2020.05.011
- [23] Wang, Y., Liu, Z., Huo, N., Li, F., Gu, M., Ling, X., . . . Ma, W. (2019). Room-temperature direct synthesis of semi-conductive PbS nanocrystal inks for optoelectronic applications. *Nat. Commun.*, 10(1). doi:10.1038/s41467-019-13158-6
- [24] Wise, F. W. (2000). Lead Salt Quantum Dots: the Limit of Strong Quantum Confinement. *Acc. Chem. Res.*, 33, 773–780.
- [25] Zhang, Y., Wu, G., Liu, F., Ding, C., Zou, Z., & Shen, Q. (2020). Photoexcited carrier dynamics in colloidal quantum dot solar cells: insights into individual quantum dots, quantum dot solid films and devices. *Chem. Soc. Rev.*, 49(1), 49-84. doi:10.1039/c9cs00560a
- [26] Zhou, Y., Itoh, H., Uemura, T., Naka, K., & Chujo, Y. (2002). Preparation, Optical Spectroscopy, and Electrochemical Studies of Novel  $\pi$ -Conjugated Polymer-Protected Stable PbS Colloidal Nanoparticles in a Nonaqueous Solution. *Langmuir*, 18, 5287–5292.